

# Entanglement dynamics for the double Tavis-Cummings model

Zhong-Xiao Man<sup>1</sup>, Yun-Jie Xia<sup>1</sup>, and Nguyen Ba An<sup>2,3</sup>

<sup>1</sup>College of Physics and Engineering, Qufu Normal University, Qufu 273165, China

<sup>2</sup>Institute of Physics and Electronics, 10 Dao Tan, Thu Le, Ba Dinh, Hanoi, Vietnam

<sup>3</sup>School of Computational Sciences, Korea Institute for Advanced Study, 207-43 Cheongryangni 2-dong, Dongdaemun-gu, Seoul 130-722, Korea

**Abstract.** A double Tavis-Cummings model (DTCM) is developed to simulate the entanglement dynamics of realistic quantum information processing where two entangled atom-pairs  $AB$  and  $CD$  are distributed in such a way that atoms  $AC$  are embedded in a cavity  $a$  while  $BD$  are located in another remote cavity  $b$ . The evolutions of different types of initially shared entanglement of atoms are studied under various initial states of cavity fields. The results obtained in the DTCM are compared with that obtained in the double Jaynes-Cummings model (DJCM) [J. Phys. B **40**, S45 (2007)] and an interaction strength theory is proposed to explain the parameter domain in which the so-called entanglement sudden death occurs for both the DTCM and DJCM.

**PACS.** 03.67.Mn Entanglement measures, witnesses, and other characterizations - 03.65.Yz Decoherence; open systems; quantum statistical methods

**QICS.** 03.30.+e Entangling power of quantum evolutions

## 1 Introduction

Entanglement is not only a key concept to distinguish between the quantum and the classical worlds, but has also been viewed as an indispensable resource to perform various intriguing global tasks in quantum computing and quantum information processing [1]. However, a notable characteristic of entanglement is its fragility in practical applications due to unavoidable interaction with the environment. It is therefore of increasing importance to understand entanglement from its dynamical behaviors in realistic systems. As a rule for a global task,

entanglement should be shared between different remote parties who participate in the task. There are cases like teleportation [2], remote state preparation [3], etc., in which each particle of a multipartite entangled state is distributed to a separate location. There are also cases in which the entangled particles should be distributed so that each location contains several particles. For example, in quantum secret communication protocol between Alice and Bob [4], an ordered  $N$  Einstein-Podolsky-Rosen (EPR) pairs are to be shared in such a way that Alice and Bob each holds one half of the pairs. That is, at Alice's location there are  $N$  particles which interact with one environment while the other  $N$  partner-particles at Bob's location collectively interact with another environment. This scenario results in two independent local environments but each of them is common for one half of the  $N$  EPR pairs. A natural question arises as to how such kind of particle-environment interactions degrade the originally prepared global entanglement. This question is of fundamental interest because any quantum protocol depends essentially on the quality of the shared entanglement. As a first step to the problem, in this paper, we consider the case of  $N = 2$  with two pairs of entangled two-level atoms  $AB$  and  $CD$  prepared in one of the two types of Bell-like states, namely,

$$|\psi(0)\rangle_{IJ} = \cos(\alpha)|10\rangle_{IJ} + \sin(\alpha)|01\rangle_{IJ}, \quad (1)$$

and

$$|\varphi(0)\rangle_{IJ} = \cos(\alpha)|11\rangle_{IJ} + \sin(\alpha)|00\rangle_{IJ}, \quad (2)$$

where  $IJ \in \{AB, CD\}$  and  $|0\rangle$  ( $|1\rangle$ ) is the atomic ground (excited) state.

For the simplest case of  $N = 1$ , i.e., either state (1) or state (2) is concerned for the initial state of a single atom-pair, the so-called double Jaynes-Cummings model (DJCM) [5-12] has been extensively adopted to study this problem because it yields exact analytical results. In the DJCM, each of two entangled atoms is embedded in an independent cavity and locally interacts with it. The results obtained within the DJCM for the initial empty cavities are that for any value of  $\alpha$  state (1) loses its entanglement only at discrete time moments  $t_l = (l + 1/2)\pi/g$  with  $l = 0, 1, 2, \dots$  and  $g$  the atom-cavity coupling constant, but for a certain domain of  $\alpha$  state (2) may become separable at times smaller than  $t_l$  and remains unentangled for some duration of time [6]. The latter phenomenon is referred to in the current literatures as entanglement sudden death (ESD) [13], which has been experimentally observed in [14,15]. An entangled state with ESD in evolution is less robust

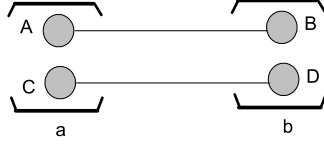


FIG. 1: Schematic representation of two entangled atom-pairs  $AB$  and  $CD$  of which atoms  $A$  and  $C$  are located in cavity  $a$  but atoms  $B$  and  $D$  in another cavity  $b$ .

than states without it, since ESD puts a limitation on the application time of entanglement. Therefore, studying ESD, especially conditions and parameter domains for its occurrence, is important from both theoretical and practical points of view. In Ref. [10] the DJCM is considered again and it is found that if the cavity fields are initially in Fock states with nonzero photon numbers then both atomic states  $|\psi(0)\rangle$  and  $|\varphi(0)\rangle$  would suffer from ESD for all values of  $\alpha$ . The DJCM was also investigated from other perspectives and it was shown that the entanglement evolution of atoms is closely related to their energy variation [9] and there is a natural entanglement invariant demonstrating the entanglement transfer among all the system's degrees of freedom [7].

For the case of  $N = 2$  involving two pairs of entangled atoms, the situation would become more complex than that of  $N = 1$ , because in each local environment there are two atoms simultaneously interacting with it. When there are many atoms interacting resonantly with a single-mode quantized radiation field of one and the same cavity the exact solution can be obtained by means of the so-called Tavis-Cummings model (TCM) [16]. Such a single TCM was used in Refs. [17] and [18] to study entanglement dynamics of two atoms that are initially prepared in a separable and entangled state, respectively. In this work we develop the so-called double Tavis-Cummings model (DTCM) including four two-level atoms  $A, B, C, D$  and two separate single-mode cavities  $a, b$  (see FIG. 1), which suffices for our purpose to study the entanglement dynamics for case of  $N = 2$ . In the DTCM, atoms  $A$  ( $C$ ) and  $B$  ( $D$ ) are initially prepared either in state (1) or (2), but atoms  $A$  and  $C$  ( $B$

and  $D$ ) are located in cavity  $a$  ( $b$ ) and interact with the cavity through the Tavis-Cummings Hamiltonian. We study the entanglement dynamics of atom-pairs  $AB$ ,  $CD$ ,  $AC$  and  $BD$  by means of concurrence in dependence on the initial entanglement type of the atoms and on the initial state of cavity fields. We compare our results obtained in the DTCM with those obtained in the DJCM and present an interaction strength theory to explain the parameter domain in which the atom-pair exhibit ESD for both the DTCM and the DJCM.

Our paper is organized as follows. In Sec. 2 we describe the DTCM and derive the exact analytical expression for the reduced density matrix of the atomic subsystem. Section 3 presents detailed analysis of atomic entanglement dynamics when the initial atom-pairs are prepared either in state (1) or state (2) and the initial cavity fields are prepared either in the vacuum state, Fock state with a non-zero photon number or the thermal state. Finally, we conclude in Sec. 4.

## 2 The double Tavis-Cummings model

The total Hamiltonian of the system of four atoms  $A, B, C, D$  and two cavities  $a, b$  (see FIG. 1) in the DTCM can be written as a sum of two isolated Tavis-Cummings Hamiltonians

$$H = H_{ACa} + H_{BDb}, \quad (3)$$

with

$$H_{ACa} = \frac{\omega_0}{2}(\sigma_A^z + \sigma_C^z) + \omega a^\dagger a + g \sum_{i=A,C} (a\sigma_i^+ + a^\dagger\sigma_i^-), \quad (4)$$

and

$$H_{BDb} = \frac{\omega_0}{2}(\sigma_B^z + \sigma_D^z) + \omega b^\dagger b + g \sum_{i=B,D} (b\sigma_i^+ + b^\dagger\sigma_i^-), \quad (5)$$

where  $\omega_0$  ( $\omega$ ) is the frequency of the atom (cavity field mode),  $a$  ( $a^\dagger$ ) is the annihilation (creation) operator of the field in cavity  $a$ ,  $b$  ( $b^\dagger$ ) is the annihilation (creation) operator of the field in cavity  $b$ ,  $\sigma_i^+ = |1\rangle_{ii}\langle 0|$  ( $\sigma_i^- = |0\rangle_{ii}\langle 1|$ ) is the rising (lowering) operator for the transition of atom  $i$  and  $g$  is the atom-cavity field coupling constant. Here, we are interested in the resonant case with  $\omega_0 = \omega$  [16]. The initial cavity fields are assumed to be either in the vacuum state, the Fock state with a non-zero photon number or the thermal state. The general thermal field with its mean photon number  $\bar{n}$  is a weighted mixture of Fock states

whose density operator  $\rho_F$  can be represented as

$$\rho_F = \sum_{n=0}^{\infty} P_n |n\rangle \langle n|, \quad (6)$$

with  $|n\rangle$  the Fock state of  $n$  photons and  $P_n$  is given by

$$P_n = \frac{\bar{n}^n}{(1 + \bar{n})^{n+1}}. \quad (7)$$

By virtue of the general thermal field defined above, through setting  $P_n = \delta_{nl}$  in Eq. (6), we can also study the vacuum state ( $l = 0$ ) as well as any Fock states ( $l > 0$ ) of the fields. As for the initial states of atom-pairs  $AB$  and  $CD$ , we assume both of them to be either in state (1) or state (2). At  $t = 0$  the total state involving the four atoms and two cavities reads

$$\rho(0) = \sum_{i,j,k,l=0}^1 \sum_{m,n=0}^{\infty} \alpha_i \alpha_j \alpha_k \alpha_l P_m^a P_n^b |ik, m\rangle_{ACaACa} \langle jl, m| \otimes |i'k', n\rangle_{BDbBDb} \langle j'l', n|, \quad (8)$$

where  $\alpha_0 \equiv \sin \alpha$ ,  $\alpha_1 \equiv \cos \alpha$  and  $i'(j', k', l') \equiv i(j, k, l) \oplus 1$  (with  $\oplus$  an addition mod 2) for state (1), while  $i'(j', k', l') \equiv i(j, k, l)$  for state (2). The evolution operator  $U_{ACa(BDb)}(t) = \exp(-iH_{ACa(BDb)}t)$  for the local interaction of atoms  $AC$  ( $BD$ ) with cavity  $a$  ( $b$ ) was derived exactly in Ref. [17]. At any time  $t > 0$  the state  $\rho(0)$  evolves into  $\rho(t) = U_{ACa}(t)U_{BDb}(t)\rho(0)U_{ACa}^\dagger(t)U_{BDb}^\dagger(t)$  which can be represented as

$$\begin{aligned} \rho(t) = & \sum_{i,j,k,l=0}^1 \sum_{m,n=0}^{\infty} \alpha_i \alpha_j \alpha_k \alpha_l P_m^a P_n^b \\ & U_{ACa}(t) |ik, m\rangle_{ACaACa} \langle jl, m| U_{ACa}^\dagger(t) \\ & \otimes U_{BDb}(t) |i'k', n\rangle_{BDbBDb} \langle j'l', n| U_{BDb}^\dagger(t). \end{aligned} \quad (9)$$

Using the analytical expression of  $U_{ACa(BDb)}(t)$  in [17] we have for  $U_{ACa} |ik, m\rangle_{ACa}$  (similarly for  $U_{BDb} |i'k', n\rangle_{BDb}$ ) :

$$U_{ACa}(t) |ik, m\rangle_{ACa} = \sum_{p,q=0}^1 X_{ik,pq}(m, \tau) |i \oplus p, k \oplus q\rangle_{AC} \left| m - (-1)^i p - (-1)^k q \right\rangle_a \quad (10)$$

where the functions  $X_{ik,pq}(m, \tau)$  with  $\tau = gt$  are given in Appendix A for various possible  $i, k, p, q$ . These functions satisfy the normalization condition

$$\sum_{p,q=0}^1 |X_{ik,pq}(m, \tau)|^2 = 1 \quad (11)$$

for any  $i, k, m$  and  $\tau$ .

The reduced density matrix  $\rho^{ABCD}(t)$  of the atomic subsystem can be obtained by tracing out  $\rho(t)$  over the cavity fields, i.e.

$$\rho^{ABCD}(t) = \text{Tr}_{ab}\rho(t) = \sum_{i,j,k,l=0}^1 \alpha_i \alpha_j \alpha_k \alpha_l \mathcal{E}_{AC}^a(|ik\rangle_{ACAC} \langle jl|) \otimes \mathcal{E}_{BD}^b(|i'k'\rangle_{BDBD} \langle j'l'|) \quad (12)$$

where  $\mathcal{E}_{XY}^c(|ik\rangle_{XYXY} \langle jl|)$ , with  $XYc = ACa$  or  $BDb$ , represents the map

$$\begin{aligned} \mathcal{E}_{XY}^c(|ik\rangle_{XYXY} \langle jl|) &\equiv \sum_{m,m'=0}^{\infty} P_m^c \langle m'| U_{XYc}(t) |ik, m\rangle_{XYcXYc} \langle jl, m| U_{XYc}^+(t) |m'\rangle \\ &= \sum_{m=0}^{\infty} \sum_{r,s,u,v=0}^1 P_m^c \delta_{(-1)^i r - (-1)^k s, (-1)^j u - (-1)^l v} \\ &\quad \times X_{ik,rs}(m, \tau) X_{jl,uv}^*(m, \tau) |i \oplus r, k \oplus s\rangle_{XYXY} \langle j \oplus u, l \oplus v|. \quad (13) \end{aligned}$$

The explicit expressions of  $\mathcal{E}_{XY}^c(|ik\rangle_{XYXY} \langle jl|)$  are given in Appendix B for various possible  $i, k, j, l$ .

### 3 Atomic entanglement dynamics

With the formulae derived in the previous section we are now in the position to analyze the entanglement dynamics of any atom-pair. By using Eq. (12) we can readily get the reduced density matrix of any pair of atoms by tracing out  $\rho^{ABCD}(t)$  over the degrees of freedom of the remaining atoms. In two-qubit domains, there exist a number of good measures of entanglement such as concurrence [19] and negativity [20]. Although the various entanglement measures may be somewhat different quantitatively [6], they are qualitatively equivalent to each other in the sense that all of them are equal to zero for unentangled states. Here we adopt Wootters' concurrence [19] because of its convenience in definition, normalization and calculation. The concurrence  $C$  for any (reduced) density matrix  $\rho$  of two qubits is defined as

$$C(\rho) = \max\{0, \sqrt{\lambda_1} - \sqrt{\lambda_2} - \sqrt{\lambda_3} - \sqrt{\lambda_4}\}, \quad (14)$$

where  $\lambda_i$  ( $\lambda_1 \geq \lambda_2 \geq \lambda_3 \geq \lambda_4$ ) are the eigenvalues of the matrix  $\zeta = \rho(\sigma_y \otimes \sigma_y) \rho^*(\sigma_y \otimes \sigma_y)$ , with  $\sigma_y$  a Pauli matrix and  $\rho^*$  the complex conjugation of  $\rho$  in the standard basis. For separate states  $C(\rho) = 0$ , whereas for maximally entangled states  $C(\rho) = 1$ . In particular,

if  $\rho$  is of the X-form [21],

$$\rho^{IJ} = \begin{pmatrix} \varrho_{11}^{IJ} & 0 & 0 & \varrho_{14}^{IJ} \\ 0 & \varrho_{22}^{IJ} & \varrho_{23}^{IJ} & 0 \\ 0 & \varrho_{32}^{IJ} & \varrho_{33}^{IJ} & 0 \\ \varrho_{41}^{IJ} & 0 & 0 & \varrho_{44}^{IJ} \end{pmatrix}, \quad (15)$$

where  $\varrho_{kk}^{IJ}$  are real positive and  $\varrho_{kl}^{IJ} = (\varrho_{lk}^{IJ})^*$  are generally complex, then the concurrence (14) simplifies to

$$C^{IJ} = 2 \max\{0, |\varrho_{23}^{IJ}| - \sqrt{\varrho_{11}^{IJ} \varrho_{44}^{IJ}}, |\varrho_{14}^{IJ}| - \sqrt{\varrho_{22}^{IJ} \varrho_{33}^{IJ}}\}. \quad (16)$$

Since both states (1) and (2) of the atoms take on and preserve the X-form in their evolution, Eq. (16) is very useful throughout this work.

### 3.1 $|\psi(0)\rangle$ type initial state for atom-pairs $AB$ and $CD$

We first consider the case when both the atom-pairs  $AB$  and  $CD$  are initially prepared in state (1). In accordance with Eq. (12) the reduced density matrix of the atomic subsystem at any time  $t$  is

$$\rho_I^{ABCD}(t) = \sum_{i,j,k,l=0}^1 \alpha_i \alpha_j \alpha_k \alpha_l \mathcal{E}_{AC}^a(|i, k\rangle_{ACAC} \langle j, l|) \otimes \mathcal{E}_{BD}^b(|i \oplus 1, k \oplus 1\rangle_{BDBD} \langle j \oplus 1, l \oplus 1|), \quad (17)$$

which can be evaluated straightforwardly via the map (13). Then the reduced density matrices of interest are  $\rho_I^{AB}(t) = \text{Tr}_{CD} \rho_I^{ABCD}(t)$ ,  $\rho_I^{CD}(t) = \text{Tr}_{AB} \rho_I^{ABCD}(t)$ ,  $\rho_I^{AC}(t) = \text{Tr}_{BD} \rho_I^{ABCD}(t)$  and  $\rho_I^{BD}(t) = \text{Tr}_{AC} \rho_I^{ABCD}(t)$ . All of  $\rho_I^{AB}(t)$ ,  $\rho_I^{CD}(t)$ ,  $\rho_I^{AC}(t)$  and  $\rho_I^{BD}(t)$  have the X-form so the corresponding concurrences are determined by Eq. (16). In the following we study the time dependence of these concurrences for the fields in cavities  $a$  and  $b$  being initially in the vacuum state, the Fock state with a non-zero photon number or the general thermal state, respectively.

In FIG.2 we plot  $C_I^{AB}$  (the same for  $C_I^{BD}$  due to symmetry) as functions of rescaled time  $gt$  and  $\alpha$  for the initial cavity fields being in the vacuum state. From FIG. 2 it is transparent that  $C_I^{AB}$  vanishes after a finite time of evolution and remains zero for some period of time before increasing again. This dynamics holds in the whole range of  $\alpha$ . A comparison between the DTCM and the DJCM [6] for the same initial preparation of the

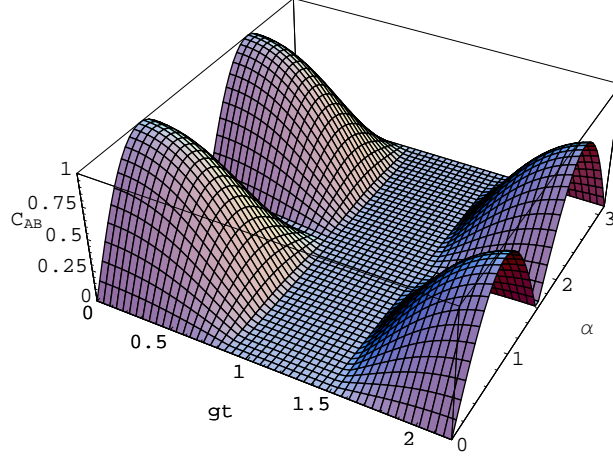


FIG. 2: The concurrence  $C_{AB} \equiv C_I^{AB}(t)$  as functions of rescaled time  $gt$  and  $\alpha$  for initially both cavity fields are in the vacuum state and both atom-pairs  $AB$  and  $CD$  are in the  $|\psi(0)\rangle(1)$  type state in the DTCM.

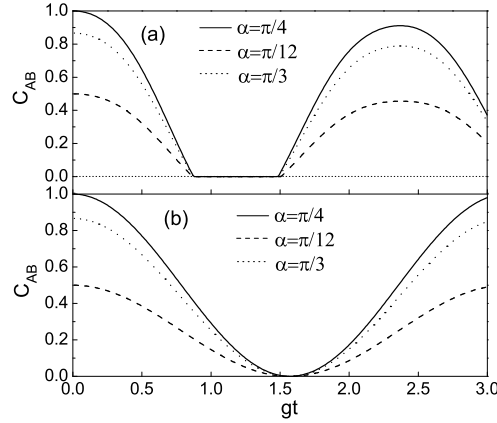


FIG. 3: The concurrence  $C_{AB} \equiv C_I^{AB}(t)$  as a function of  $gt$  for various values of  $\alpha$  for the same initial preparation of cavities and atoms as in Fig. 2 in (a) the DTCM and (b) the DJCM.

cavities and atoms is shown in FIG. 3. Within the first cycle of evolution, in the DJCM (see FIG. 3b)  $C_I^{AB}$  vanishes at the moment  $t_0 = \pi/(2g)$  and grows up again right after  $t_0$ , while in the DTCM (see FIG. 3a)  $C_I^{AB} = 0$  at a time shorter than  $t_0$  and remains so for some time before reviving. This indicates that for one and the same empty cavity fields,  $|\psi(0)\rangle$  type initial state of atoms does not undergo ESD in the DJCM but it does in the DTCM. Therefore, the atomic entanglement dynamics is model-dependent apart from the



entanglement type itself. The physical interpretation behind such a clear distinction in the dynamical behaviors between the two models can be thought of as follows. If the cavities are empty, atoms in the ground state  $|0\rangle$  remain unchanged and only atoms in the excited state  $|1\rangle$  can interact with the cavity fields. Denoting by  $N_{|1\rangle}$  the number of atoms that may be populated in state  $|1\rangle$ , the system-environment interaction can be classified into two regimes, “strong” and “weak” interaction regimes, depending on relative magnitudes of  $P_{\geq}$  and  $P_{<}$ , where  $P_{\geq}$  ( $P_{<}$ ) is the probability that  $N_{|1\rangle} \geq N_c$  ( $N_{|1\rangle} < N_c$ ) with  $N_c$  the number of cavities. In the DTCM considered here and the DJCM considered in [6,7] it is clear that  $N_c = 2$ . We define the following convention: the strong interaction regime corresponds to  $P_{\geq} > P_{<}$ , while  $P_{\geq} \leq P_{<}$  implies the weak interaction regime. In the DJCM the total system state of two atoms  $A, B$  and two cavities  $a, b$  at  $t = 0$  reads

$$|\psi(0)\rangle_{AB} |00\rangle_{ab} = \cos \alpha |10\rangle_{Aa} |00\rangle_{Bb} + \sin \alpha |00\rangle_{Aa} |10\rangle_{Bb}, \quad (18)$$

whereas in the DTCM the total system state of four atoms  $A, B, C, D$  and two cavities  $a, b$  at  $t = 0$  reads

$$\begin{aligned} |\psi(0)\rangle_{AB} |\psi(0)\rangle_{CD} |00\rangle_{ab} = & \cos^2 \alpha |110\rangle_{ACa} |000\rangle_{BDb} + \cos \alpha \sin \alpha |100\rangle_{ACa} |010\rangle_{BDb} \\ & + \sin \alpha \cos \alpha |010\rangle_{ACa} |100\rangle_{BDb} + \sin^2 \alpha |000\rangle_{ACa} |110\rangle_{BDb} \end{aligned} \quad (19)$$

From Eq. (18) it follows that there is always only one atom (namely, either atom  $A$  in the first term or atom  $B$  in the second term) being in state  $|1\rangle$  regardless of the value of  $\alpha$ . That is,  $P_{<} = 1 < P_{\geq} = 0$ , resulting in the weak interaction regime in the DJCM for the whole range of  $\alpha$ . However, what is followed from Eq. (19) is that for any value of  $\alpha$  there are always two atoms (namely, either atoms  $A$  and  $C$  in the first term or atoms  $A$  and  $D$  in the second term or atoms  $C$  and  $B$  in the third term or atoms  $B$  and  $D$  in the fourth term) being in state  $|1\rangle$ . That is,  $P_{\geq} = 1 > P_{<} = 0$ , resulting in the strong interaction regime in the DTCM regardless of the value of  $\alpha$ . Therefore, it can be said that, when the cavities are initially prepared in the vacuum state,  $|\psi(0)\rangle$  type initial state of atoms exhibits ESD in the strong interaction regime (i.e., in the DTCM) but it does not in the weak interaction regime (i.e., in the DJCM), independent of the parameter  $\alpha$ .

The case when the initial cavity fields are in a Fock state with a certain nonzero photon number is illustrated in FIG. 4. In this case not only atoms in state  $|1\rangle$  but also atoms in state  $|0\rangle$ , i.e., all the present atoms, can interact with the cavity fields so that the interaction

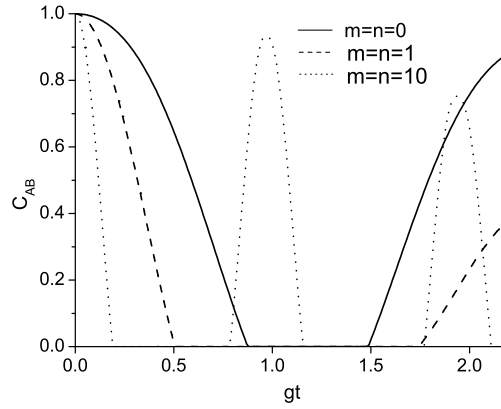


FIG. 4: The concurrence  $C_{AB} \equiv C_I^{AB}(t)$  as a function of  $gt$  for  $\alpha = \pi/4$  for initially the cavity fields are in different Fock states  $|mn\rangle_{ab}$  and atom-pairs  $AB$  and  $CD$  are in the  $|\psi(0)\rangle$  (1) type state in the DTCM.

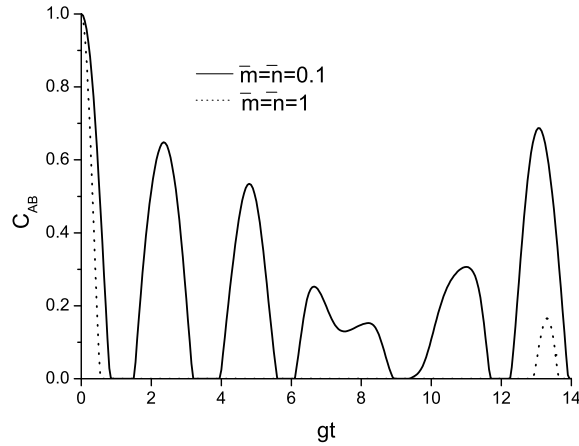


FIG. 5: The concurrence  $C_{AB} \equiv C_I^{AB}(t)$  as a function of  $gt$  for  $\alpha = \pi/4$  for initially cavity fields are in the thermal state with different mean photon numbers  $\bar{m}, \bar{n}$  and atom-pairs  $AB$  and  $CD$  are in the  $|\psi(0)\rangle$  (1) type state in the DTCM.

regime is always strong resulting in ESD for whatever values of  $\alpha$ . A remarkable feature is that  $C_I^{AB}$  decays quicker and reaches zero in a shorter time for a larger initial number of photons in the cavities. The underlying physics for that feature is the intensification of the system-environment effective interaction with the increase of photon number contained in the cavities.

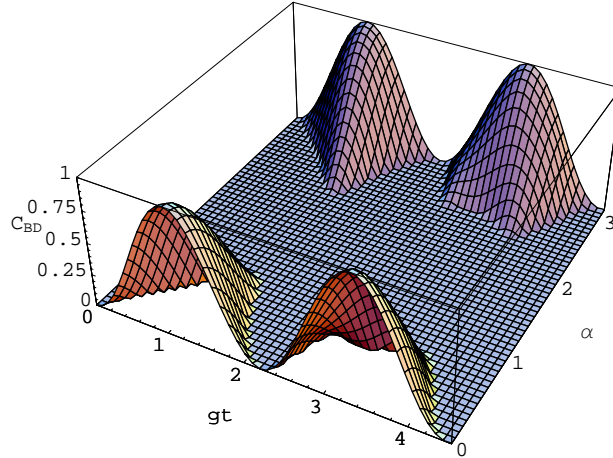


FIG. 6: The concurrence  $C_{BD} \equiv C_I^{BD}(t)$  as functions of  $gt$  and  $\alpha$  for initially the cavity fields are in the Fock state  $|11\rangle_{ab}$  and both atom-pairs  $AB$  and  $CD$  are in the state (1) in the DTCM.

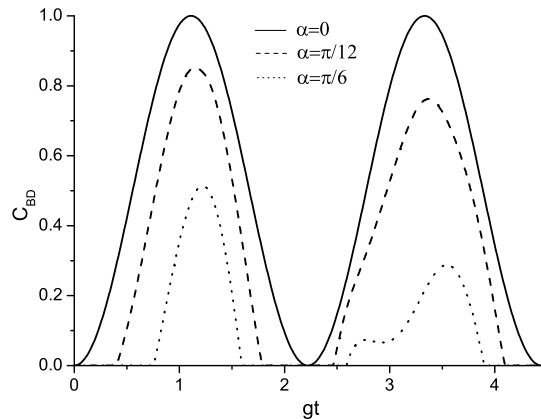


FIG. 7: The concurrence  $C_{BD} \equiv C_I^{BD}(t)$  as a function of  $gt$  for various values of  $\alpha$  with the same initial preparation of cavity fields and atom-pairs as in Fig. 6 in the DTCM.

Figure 5 plots the evolution of  $C_I^{AB}$  for the cavity fields being initially in the thermal state. The entanglement dynamics looks chaotic due to the nature of the thermal fields. As can be seen from FIG. 5, the larger the mean photon number (corresponding to the higher temperature) the shorter the death time of  $C_I^{AB}$  and the longer its revival time.

At this point let us study the dynamics of the two atoms that are located in one and the same cavity. These are atoms  $A$  and  $C$  in cavity  $a$  and atoms  $B$  and  $D$  in cavity  $b$ . Such atoms in the same cavity are absolutely uncorrelated at the beginning and also there are no

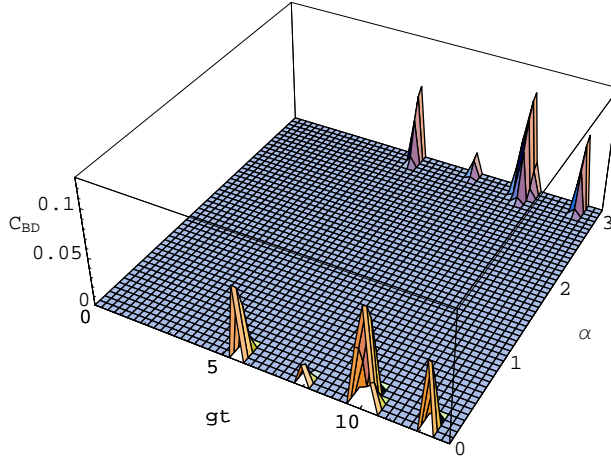


FIG. 8: The concurrence  $C_{BD} \equiv C_I^{BD}(t)$  as functions of  $gt$  and  $\alpha$  for initially the cavity fields are in the thermal state with the mean photon numbers  $\bar{n} = \bar{n} = 1$  and both atom-pairs  $AB$  and  $CD$  are in the state (1) in the DTCM.

direct interactions between them during the entire course of evolution, in accordance with the problem Hamiltonians (4) and (5). However, an effective (indirect) atom-atom interaction is induced for  $t > 0$  thanks to the coupling of both atoms with a common environment. Such an effective atom-atom interaction could nontrivially affect their global behaviors. In fact, as investigated in Ref. [17], if the initial atoms are prepared either in state  $|01\rangle$  or  $|10\rangle$  ( $|11\rangle$ ), then they always get entangled with each other (remain unentangled) regardless of the nature of the cavity fields. But, if the atomic initial state is  $|00\rangle$ , then the field in the vacuum state leaves the atoms unentangled and the field in a Fock state with a non-zero photon number or thermal state can entangle them. Here, in the DTCM, at variance with the situation considered in Ref. [17], at  $t = 0$  the atoms in a cavity, though being independent of each other, are entangled with other atoms in another cavity. That is, we have at  $t = 0$  in cavity  $a$  ( $b$ ) a mixed state  $\rho_I^{AC}(0) = \text{Tr}_{BD}\rho_I^{ABCD}(0) = \sum_{i,j=0}^1 \alpha_i^2 \alpha_j^2 |i, j\rangle_{ACAC} \langle i, j|$  ( $\rho_I^{BD}(0) = \text{Tr}_{AC}\rho_I^{ABCD}(0) = \sum_{i,j=0}^1 \alpha_i^2 \alpha_j^2 |i \oplus 1, j \oplus 1\rangle_{BDBD} \langle i \oplus 1, j \oplus 1|$ ), instead of a pure state as in Ref. [17]. Figure 6 plots the concurrence  $C_I^{BD}$  as functions of  $gt$  and  $\alpha$  with the initial fields in both cavities containing just one photon. This figure shows that the entanglement dynamics of the atoms is sensitive to  $\alpha$ , as it should be. For example, in the region of  $\alpha \in [0, 0.29\pi]$  atoms  $B$  and  $D$  can get entangled, but for  $\alpha$  around  $\pi/2$  no entanglement is generated through the whole evolution. These results are in full agreement

with those reported in Ref. [17] where  $\alpha = 0$  (i.e.,  $\rho_I^{BD}(0) = |00\rangle_{BDBD} \langle 00|$ ) and  $\alpha = \pi/2$  (i.e.,  $\rho_I^{BD}(0) = |11\rangle_{BDBD} \langle 11|$ ) are concerned. To get more insight into the effect of  $\alpha$  on atomic entanglement generation we show in FIG. 7 a 2D plot of  $C_I^{BD}$  as a function of  $gt$  with the initial cavity fields in the Fock states  $|1, 1\rangle_{ab}$  for various values of  $\alpha$ . When  $\alpha = 0$  (i.e.,  $\rho_I^{BD}(0) = |00\rangle_{BDBD} \langle 00|$ ), the entanglement of  $B$  and  $D$  emerges immediately from  $t = 0$ . Nevertheless, when  $\alpha > 0$  the atoms remain unentangled for some initial period of time and suddenly become entangled at some later time. The larger the value of  $\alpha$  the longer the delay time of entanglement generation. Such phenomena of delayed entanglement during the time evolution can be called “entanglement sudden birth” (ESB) [22]. The effect of thermal fields on inducing entanglement between atoms  $B$  and  $D$  is drawn in FIG. 8 with the cavity mean photon numbers  $\bar{m} = \bar{n} = 1$ , which agrees well with the result in Ref. [17] for  $\alpha = 0$ . Since the thermal state is a weighted mixture of Fock states (see Eq. (6)), it is a chaotic state with minimum information and so its effect is generally irregular. In comparison with the case of “corresponding” Fock states  $|1, 1\rangle_{ab}$  one sees that the region of  $\alpha$  allowing entanglement of atoms is much shrunk and the amount of generated entanglement is very small. The plots of  $C_I^{AC}$  can be obtained from those of  $C_I^{BD}$  by making a change  $\alpha \rightarrow \alpha + \pi/2$ .

### 3.2 $|\varphi(0)\rangle$ type initial state for atom-pairs $AB$ and $CD$

We next consider the case when both atom-pairs  $AB$  and  $CD$  are initially prepared in state (2). In accordance with Eq. (12) the reduced density matrix of the atomic subsystem at any time  $t$  is

$$\rho_{II}^{ABCD}(t) = \sum_{i,j,k,l=0}^1 \alpha_i \alpha_j \alpha_k \alpha_l \mathcal{E}_{AC}^a(|i, k\rangle_{ACAC} \langle j, l|) \otimes \mathcal{E}_{BD}^b(|i, k\rangle_{BDBD} \langle j, l|). \quad (20)$$

In FIG.9 we plot  $C_{II}^{AB}$  (the same for  $C_{II}^{BD}$  due to symmetry) versus  $gt$  and  $\alpha$  for the initial empty cavity fields. It is visual from this figure that ESD occurs but not in the whole range of  $\alpha$ , in clear contrast with the case shown in FIG. 2 when both the atom-pairs  $AB$  and  $CD$  are initially prepared in state (1). To derive the constraint on  $\alpha$  that triggers ESD let us look at the total system state at  $t = 0$ :

$$\begin{aligned} |\varphi(0)\rangle_{AB} |\varphi(0)\rangle_{CD} |00\rangle_{ab} = & \cos^2 \alpha |110\rangle_{ACa} |110\rangle_{BDb} + \cos \alpha \sin \alpha |100\rangle_{ACa} |100\rangle_{BDb} \\ & + \sin \alpha \cos \alpha |010\rangle_{ACa} |010\rangle_{BDb} + \sin^2 \alpha |000\rangle_{ACa} |000\rangle_{BDb} \end{aligned} \quad (21)$$

Obviously, the probability that all the four atoms are in state  $|1\rangle$  is  $\cos^4 \alpha$ , the probability that only two atoms (namely, either atoms  $A$  and  $B$  or atoms  $C$  and  $D$ ) are in state  $|1\rangle$  is  $2 \cos^2 \alpha \sin^2 \alpha$  and the probability that none of the atoms are in state  $|1\rangle$  (i.e., all the atoms are in state  $|0\rangle$ ) is  $\sin^4 \alpha$ . That is,  $P_{\geq} = \cos^4 \alpha + 2 \cos^2 \alpha \sin^2 \alpha$  and  $P_{<} = \sin^4 \alpha$ . As mentioned in the previous subsection, the condition for the occurrence of ESD is that the interaction regime is strong, i.e.,  $P_{\geq} > P_{<}$ . So, the values of  $\alpha$  for which ESD occurs should satisfy the constraint

$$\sin^2 \alpha < \frac{1}{\sqrt{2}}. \quad (22)$$

Noticeably, this constraint is not coincident with that one in the DJCM for which the initial total system state reads

$$|\varphi(0)\rangle_{AB} |00\rangle_{ab} = \cos \alpha |10\rangle_{Aa} |10\rangle_{Bb} + \sin \alpha |00\rangle_{Aa} |00\rangle_{Bb}. \quad (23)$$

As followed from Eq. (23), the probability that the two atoms are in state  $|1\rangle$  is  $\cos^2 \alpha$  and the probability that none of the atoms are in state  $|1\rangle$  is  $\sin^2 \alpha$ . That is,  $P_{\geq} = \cos^2 \alpha$ ,  $P_{<} = \sin^2 \alpha$  and thus the values of  $\alpha$ , for which the system-environment interaction regime is strong (i.e., ESD occurs) in the DJCM, satisfy the constraint

$$\sin^2 \alpha < \frac{1}{2}. \quad (24)$$

The constraints (22) and (24) imply that the  $\alpha$ -parameter domain in which the atoms suffer from ESD is wider in the DTTCM than in the DJCM.

The case for the initial cavity fields being in a Fock state  $|11\rangle_{ab}$  is plotted in FIG. 10. A remarkable feature as compared with the vacuum fields case in FIG. 9 is that here ESD occurs in the whole range of  $\alpha$ . Again, the physical reason for this is that in the presence of initial photons all the atoms are in interaction with the cavity fields (i.e., not only atoms in state  $|1\rangle$  but also those in state  $|0\rangle$  interact with the cavity fields).

In FIG. 11 we plot  $C_{II}^{AB}$  as a function of  $gt$  for the initial fields in a thermal state with different mean photon numbers for a given value of  $\alpha$ . Comparing FIG. 11 with FIG. 5 signals that with relatively small mean photon numbers (e.g.,  $\overline{m} = \overline{n} = 0.1$ ) the signature of ESD is less pronounced for the case when the initial atoms are prepared in state (2) than in state (1).

The entanglement generation dynamics of the atomic pairs  $AC$  and  $BD$  is similar to the case considered in the preceding subsection and thus will not be iterated here.

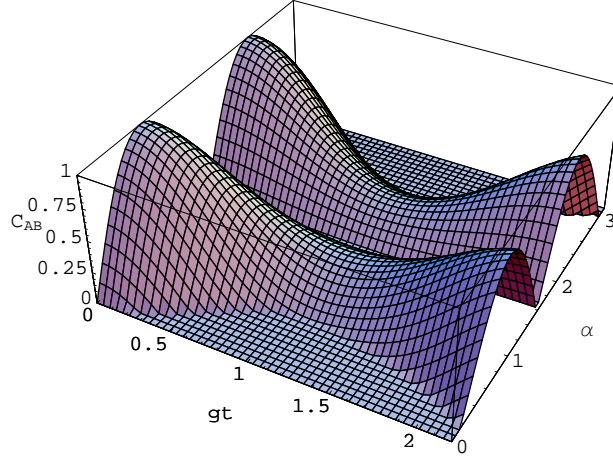


FIG. 9: The concurrence  $C_{AB} \equiv C_{II}^{AB}(t)$  as functions of  $gt$  and  $\alpha$  for initially both cavity fields are in the vacuum state and both atom-pairs  $AB$  and  $CD$  are in the  $|\varphi(0)\rangle$  (2) type state in the DTCM.

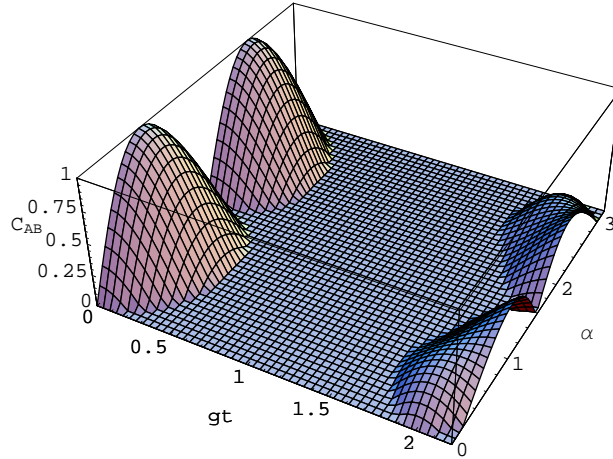


FIG. 10: The concurrence  $C_{AB} \equiv C_{II}^{AB}(t)$  as functions of  $gt$  and  $\alpha$  for initially the cavity fields are in the Fock state  $|11\rangle_{ab}$  and both atom-pairs  $AB$  and  $CD$  are in the  $|\varphi(0)\rangle$  (2) type state in the DTCM.

#### 4 Conclusion

In conclusion, we have, by means of concurrence, studied the entanglement dynamics of the DTCM motivated by certain realistic quantum information processing. The system is composed of four two-level atoms  $A, B, C, D$  and two spatially separated single-mode cavities

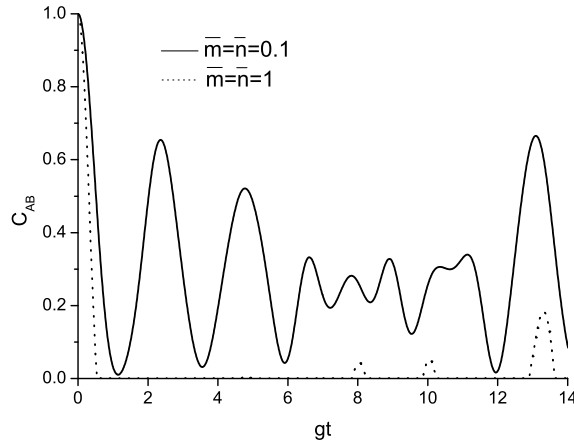


FIG. 11: The concurrence  $C_{AB} \equiv C_{II}^{AB}(t)$  as a function of  $gt$  for  $\alpha = \pi/4$  for initially the cavity fields are in the thermal state with different mean photon numbers  $\bar{m}, \bar{n}$  and both atom-pairs  $AB$  and  $CD$  are in the  $|\varphi(0)\rangle$  (2) type state in the DTCM.

*a, b.* Initially, atom-pairs  $AB$  and  $CD$  are prepared either in Bell-like state  $|\psi(0)\rangle$  (1) or  $|\varphi(0)\rangle$  (2), while both cavities are prepared either in the vacuum state, the Fock state with non-zero photon numbers or the thermal state. Independent atoms  $A, C$  ( $B, D$ ) that belong to different entangled atom-pairs are embedded in one and the same cavity  $a$  ( $b$ ) and interact with it through the Tavis-Cummings Hamiltonian.

For the vacuum fields the  $|\psi(0)\rangle$  type initial state of atom-pairs  $AB$  and  $CD$  displays ESD for the whole value range of the parameter  $\alpha$  which represents the initial entanglement degree of  $AB$  and  $CD$ . This result is in sharp contrast with the DJCM for which ESD does not occur at all for whatever values of  $\alpha$  [6,7]. As for the  $|\varphi(0)\rangle$  type initial state of atom-pairs  $AB$  and  $CD$ , ESD only occurs for the value of  $\alpha$  such that  $\sin^2 \alpha < 1/\sqrt{2}$ , which is wider than that in the DJCM where ESD occurs just for  $\alpha$  such that  $\sin^2 \alpha < 1/2$  [6,7]. Physically, these results (i.e., the domain of  $\alpha$  for which ESD occurs) in both the DTCM and DJCM can be explained via the interaction strength theory according to which ESD occurs (does not occur) in the strong (weak) system-environment interaction regime. The interaction regime is identified by the number of atoms that can have interaction with the cavities, which is determined by the relative magnitudes of  $P_{\geq}$  and  $P_{<}$  defined in subsection 3.1. Remarkably, the interaction strength theory turns out to apply also for the so-called triple Jaynes-Cummings model [23] for GHZ-like atomic states as well as for the case of



multiple dissipative environments with multiqubit GHZ-like atomic states [24,25].

We have shown that the non-vacuum environments of cavities have great effects on the appearance of ESD for atoms. That is, when the cavity fields are initially in the Fock state with a non-zero photon number or the general thermal state, ESD always happens for atom-pairs  $AB$  and  $CD$  regardless of the entanglement type they are prepared. Moreover, the more photon number in the Fock state or the greater the mean photon number in the thermal state the quicker the entanglement decay rate, i.e., the sooner the time of ESD occurrence. In terms of the interaction strength theory, these properties are explained by the physical fact that in the presence of nonzero (mean) photon number the interaction regime is always strong because all the atoms (i.e., not only those in the excited state as in the case of empty cavities) can interact with the fields. Thus, the actual system-environment interaction strength is now identified by the number of excitation which in these cases is proportional to the total number of both atoms and photons.

We have also studied creation of entanglement between initially uncorrelated atoms  $A$  and  $C$  in cavity  $a$  ( $B$  and  $D$  in cavity  $b$ ). Compared to the case of  $\alpha = 0$  considered in Ref. [17] here we showed that for  $\alpha \neq 0$  there appears the so-called entanglement sudden birth, i.e., the formation of atomic entanglement does not take place at once as the system evolves but emerges suddenly at some delayed time, which is dependent on the value of  $\alpha$ . The DTCM presented in this work could be extended to the general multiple case where two groups of multipartite entangled atoms are distributed in such a way that every two atoms from different group are located in the same environment. In this way, we can study not only the pairwise entanglement of atoms between any two nodes (cavities or local environments) via concurrence but also the entanglement of any atomic bipartition by means of negativity. These studies can reveal the degraded properties of various multipartite entangled state and thus be useful for the large-scale quantum information processing.

Z.X.M. and Y.J.X. are supported by National Natural Science Foundation of China under Grant No. 10774088. N.B.A. acknowledges support from a NAFOSTED project No. NCCB-2009 and from the KIAS Scholar program.

### APPENDIX A: THE EXPLICIT EXPRESSIONS OF $X_{ik,pq}(m, \tau)$

The functions  $X_{ik,pq}(m, \tau)$  appearing in Eq. (10) for all possible  $i, k, p, q$  are given by

$$X_{11,00}(m, \tau) = \frac{m+1}{2m+3} [\cos(\sqrt{2(2m+3)}\tau) - 1] + 1, \quad (\text{A1})$$

$$X_{11,10}(m, \tau) = X_{11,01}(m, \tau) = -i\sqrt{\frac{m+1}{2(2m+3)}} \sin(\sqrt{2(2m+3)}\tau), \quad (\text{A2})$$

$$X_{11,11}(m, \tau) = \frac{\sqrt{(m+1)(m+2)}}{2m+3} [\cos(\sqrt{2(2m+3)}\tau) - 1], \quad (\text{A3})$$

$$X_{01,10}(m, \tau) = X_{10,01}(m, \tau) = -i\sqrt{\frac{m}{2(2m+1)}} \sin(\sqrt{2(2m+1)}\tau), \quad (\text{A4})$$

$$X_{01,00}(m, \tau) = X_{10,00}(m, \tau) = \frac{1}{2} [\cos(\sqrt{2(2m+1)}\tau) + 1], \quad (\text{A5})$$

$$X_{01,11}(m, \tau) = X_{10,11}(m, \tau) = \frac{1}{2} [\cos(\sqrt{2(2m+1)}\tau) - 1], \quad (\text{A6})$$

$$X_{01,01}(m, \tau) = X_{10,10}(m, \tau) = -i\sqrt{\frac{m+1}{2(2m+1)}} \sin(\sqrt{2(2m+1)}\tau), \quad (\text{A7})$$

$$X_{00,11}(m, \tau) = \frac{\sqrt{m(m-1)}}{2m-1} [\cos(\sqrt{2(2m-1)}\tau) - 1], \quad (\text{A8})$$

$$X_{00,01}(m, \tau) = X_{00,10}(m, \tau) = -i\sqrt{\frac{m}{2(2m-1)}} \sin(\sqrt{2(2m-1)}\tau) \quad (\text{A9})$$

and

$$X_{00,00}(m, \tau) = \frac{m}{2m-1} [\cos(\sqrt{2(2m-1)}\tau) - 1] + 1. \quad (\text{A10})$$

### APPENDIX B: THE EXPLICIT EXPRESSIONS OF $\mathcal{E}_{XY}^c(|ik\rangle_{XYXY}\langle jl|)$

The expressions of the map  $\mathcal{E}_{XY}^c(|ik\rangle_{XYXY}\langle jl|)$ , with  $XYc = ACa$  or  $BDb$ , appearing in Eq. (13) for all possible  $i, k, j, l$  are given by

$$\begin{aligned} \mathcal{E}_{XY}^c(|00\rangle_{XYXY}\langle 00|) = & \sum_{m=0}^{\infty} P_m^c \left[ |X_{00,11}(m, \tau)|^2 |11\rangle_{XYXY}\langle 11| \right. \\ & + |X_{00,10}(m, \tau)|^2 |10\rangle_{XYXY}\langle 10| \\ & + X_{00,10}(m, \tau) X_{00,01}^*(m, \tau) |10\rangle_{XYXY}\langle 01| \\ & + X_{00,01}(m, \tau) X_{00,10}^*(m, \tau) |01\rangle_{XYXY}\langle 10| \\ & + |X_{00,01}(m, \tau)|^2 |01\rangle_{XYXY}\langle 01| \\ & \left. + |X_{00,00}(m, \tau)|^2 |00\rangle_{XYXY}\langle 00| \right], \quad (\text{B1}) \end{aligned}$$

$$\begin{aligned}
\mathcal{E}_{XY}^c(|01\rangle_{XYXY}\langle 00|) &= \mathcal{E}_{XY}^c(|00\rangle_{XYXY}\langle 01|)^* \\
&= \sum_{m=0}^{\infty} P_m^c \left[ X_{01,10}(m, \tau) X_{00,01}^*(m, \tau) |11\rangle_{XYXY} (\langle 01| + \langle 10|) | \right. \\
&\quad + X_{01,11}(m, \tau) X_{00,00}^*(m, \tau) |10\rangle_{XYXY} \langle 00| \\
&\quad \left. + X_{01,00}(m, \tau) X_{00,00}^*(m, \tau) |01\rangle_{XYXY} \langle 00| \right], \tag{B2}
\end{aligned}$$

$$\begin{aligned}
\mathcal{E}_{XY}^c(|10\rangle_{XYXY}\langle 00|) &= \mathcal{E}_{XY}^c(|00\rangle_{XYXY}\langle 10|)^* \\
&= \sum_{m=0}^{\infty} P_m^c \left[ X_{10,01}(m, \tau) X_{00,10}^*(m, \tau) |11\rangle_{XYXY} \langle 10| \right. \\
&\quad + X_{10,01}(m, \tau) X_{00,01}^*(m, \tau) |11\rangle_{XYXY} \langle 01| \\
&\quad + X_{10,00}(m, \tau) X_{00,00}^*(m, \tau) |10\rangle_{XYXY} \langle 00| \\
&\quad \left. + X_{10,11}(m, \tau) X_{00,00}^*(m, \tau) |01\rangle_{XYXY} \langle 00| \right], \tag{B3}
\end{aligned}$$

$$\begin{aligned}
\mathcal{E}_{XY}^c(|11\rangle_{XYXY}\langle 00|) &= \mathcal{E}_{XY}^c(|00\rangle_{XYXY}\langle 11|)^* \\
&= \sum_{m=0}^{\infty} P_m^c X_{11,00}(m, \tau) X_{00,00}^*(m, \tau) |11\rangle_{XYXY} \langle 00|, \tag{B4}
\end{aligned}$$

$$\begin{aligned}
\mathcal{E}_{XY}^c(|01\rangle_{XYXY}\langle 01|) &= \sum_{m=0}^{\infty} P_m^c \left[ |X_{01,10}(m, \tau)|^2 |11\rangle_{XYXY} \langle 11| \right. \\
&\quad + X_{01,11}(m, \tau) X_{01,00}^*(m, \tau) |10\rangle_{XYXY} \langle 01| \\
&\quad + |X_{01,11}(m, \tau)|^2 |10\rangle_{XYXY} \langle 00| \\
&\quad + X_{01,00}(m, \tau) X_{01,11}^*(m, \tau) |01\rangle_{XYXY} \langle 10| \\
&\quad + |X_{01,00}(m, \tau)|^2 |01\rangle_{XYXY} \langle 01| \\
&\quad \left. + |X_{01,01}(m, \tau)|^2 |00\rangle_{XYXY} \langle 00| \right], \tag{B5}
\end{aligned}$$

$$\begin{aligned}
\mathcal{E}_{XY}^c(|10\rangle_{XYXY}\langle 01|) &= \mathcal{E}_{XY}^c(|01\rangle_{XYXY}\langle 10|)^* \\
&= \sum_{m=0}^{\infty} P_m^c \left[ |X_{10,01}(m, \tau)|^2 |11\rangle_{XYXY} \langle 11| \right. \\
&\quad + X_{10,00}(m, \tau) X_{01,11}^*(m, \tau) |10\rangle_{XYXY} \langle 10| \\
&\quad + |X_{10,00}(m, \tau)|^2 |10\rangle_{XYXY} \langle 01| \\
&\quad + |X_{10,11}(m, \tau)|^2 |01\rangle_{XYXY} \langle 10| \\
&\quad + X_{10,11}(m, \tau) X_{01,00}^*(m, \tau) |01\rangle_{XYXY} \langle 01| \\
&\quad \left. + |X_{10,10}(m, \tau)|^2 |00\rangle_{XYXY} \langle 00| \right], \tag{B6}
\end{aligned}$$

$$\begin{aligned}
\mathcal{E}_{XY}^c(|11\rangle_{XYXY}\langle 01|) &= \mathcal{E}_{XY}^c(|01\rangle_{XYXY}\langle 11|)^* \\
&= \sum_{m=0}^{\infty} P_m^c \left[ X_{11,00}(m, \tau) X_{01,11}^*(m, \tau) |11\rangle_{XYXY}\langle 10| \right. \\
&\quad + X_{11,00}(m, \tau) X_{01,00}^*(m, \tau) |11\rangle_{XYXY}\langle 01| \\
&\quad + X_{11,01}(m, \tau) X_{01,01}^*(m, \tau) |10\rangle_{XYXY}\langle 00| \\
&\quad \left. + X_{11,10}(m, \tau) X_{01,01}^*(m, \tau) |01\rangle_{XYXY}\langle 00| \right], \tag{B7}
\end{aligned}$$

$$\begin{aligned}
\mathcal{E}_{XY}^c(|10\rangle_{XYXY}\langle 10|) &= \sum_{m=0}^{\infty} P_m^c \left[ |X_{10,01}(m, \tau)|^2 |11\rangle_{XYXY}\langle 11| \right. \\
&\quad + |X_{10,00}(m, \tau)|^2 |10\rangle_{XYXY}\langle 10| \\
&\quad + X_{10,00}(m, \tau) X_{10,11}^*(m, \tau) |10\rangle_{XYXY}\langle 01| \\
&\quad + X_{10,11}(m, \tau) X_{10,00}^*(m, \tau) |01\rangle_{XYXY}\langle 10| \\
&\quad + |X_{10,11}(m, \tau)|^2 |01\rangle_{XYXY}\langle 01| + \\
&\quad \left. |X_{10,10}(m, \tau)|^2 |00\rangle_{XYXY}\langle 00| \right], \tag{B8}
\end{aligned}$$

$$\begin{aligned}
\mathcal{E}_{XY}^c(|11\rangle_{XYXY}\langle 10|) &= \mathcal{E}_{XY}^c(|10\rangle_{XYXY}\langle 11|)^* \\
&= \sum_{m=0}^{\infty} P_m^c \left[ X_{11,00}(m, \tau) X_{10,00}^*(m, \tau) |11\rangle_{XYXY}\langle 10| \right. \\
&\quad + X_{11,00}(m, \tau) X_{10,11}^*(m, \tau) |11\rangle_{XYXY}\langle 01| \\
&\quad + X_{11,01}(m, \tau) X_{10,10}^*(m, \tau) |10\rangle_{XYXY}\langle 00| \\
&\quad \left. + X_{11,10}(m, \tau) X_{10,10}^*(m, \tau) |01\rangle_{XYXY}\langle 00| \right] \tag{B9}
\end{aligned}$$

and

$$\begin{aligned}
\mathcal{E}_{XY}^c(|11\rangle_{XYXY}\langle 11|) &= \sum_{m=0}^{\infty} P_m^c \left[ |X_{11,00}(m, \tau)|^2 |11\rangle_{XYXY}\langle 11| \right. \\
&\quad + |X_{11,01}(m, \tau)|^2 (|10\rangle + |01\rangle)_{XYXY} (\langle 10| + \langle 01|) \\
&\quad \left. + |X_{11,11}(m, \tau)|^2 |00\rangle_{XYXY}\langle 00| \right]. \tag{B10}
\end{aligned}$$

## References

1. M. A. Nielsen and I. L. Chuang, Quantum Computation and Quantum Information (Cambridge University Press. Cambridge, 2000)
2. C. H. Bennett et al., Phys. Rev. Lett. **70**, 1895 (1993)

3. A. K. Pati, Phys. Rev. A **63**, 014302 (2000)
4. F. G. Deng, G. L. Long and X. S. Liu, Phys. Rev. A **68**, 042317 (2003)
5. M. Yönaç, T. Yu and J. H. Eberly, J. Phys. B **39**, S621 (2006)
6. M. Yönaç, T. Yu T and J. H. Eberly, J. Phys. B **40**, S45 (2007)
7. I. Sainz and G. Björk, Phys. Rev. A **76**, 042313 (2007)
8. J. G. Oliveira, R. Rossi, and M. C. Nemes, Phys. Rev. A **78**, 044301 (2008)
9. D. Cavalcanti, et al., Phys. Rev. A **74**, 042328 (2006)
10. Z. X. Man, Y. J. Xia, and Nguyen Ba An, J. Phys. B **41**, 085503 (2008)
11. J. H. Cole, e-print arXiv:quant-ph/0809.1746v1
12. S. Chan, M. D. Reid, and Z. Ficek, e-print arXiv:quant-ph/0810.3050v1
13. T. Yu and J. H. Eberly, Phys. Rev. Lett. **97**, 140403 (2006);  
J. H. Eberly and T. Yu, Science **316**, 555 (2007);  
B. Bellomo, R. Lo Franci and G. Compagno, Phys. Rev. Lett. **99**, 160502 (2007)
14. Almeida M P, *et al.*, Science **316**, 579 (2007)
15. J. Laurat, K. S. Choi, H. Deng, C. W. Chou, H. J. Kimble, Phys. Rev. Lett. **99**, 180504 (2007)
16. M. Tavis and F. W. Cummings, Phys. Rev. **170**, 379 (1968)
17. M. S. Kim, J. Lee, D. Ahn, and P. L. Knight, Phys. Rev. A **65**, 040101(R) (2002)
18. H. T. Cui, K. Li, and X. X. Yi, Phys. Lett. A **365**, 44 (2007)
19. W. K. Wootters, Phys. Rev. Lett. **80**, 2245 (1998)
20. G. Vidal and R. F. Werner, Phys. Rev. A **65**, 032314(2002);  
K. Audenaert, M. B. Plenio, and J. Eisert, Phys. Rev. Lett. **90**, 027901 (2003)
21. T. Yu and J. H. Eberly, Quantum Inf. Comput. **7**, 459 (2007)
22. C. E. López, *et al.*, Phys. Rev. Lett. **101**, 080503 (2008);  
M. Abdel-Aty, T. Yu, J. Phys. B **41**, 235503 (2008);  
Z. Ficek and R. Tanas, Phys. Rev. A **77**, 054301 (2008)
23. Z. X. Man, Y. J. Xia, and Nguyen Ba An, J. Phys. B **41**, 155501 (2008)
24. L. Aolita, R. Chaves, D. Cavalcanti, A. Acín, and L. Davidovich, Phys. Rev. Lett. **100**, 080501 (2008)
25. Z. X. Man, Y. J. Xia, and Nguyen Ba An, Phys. Rev. A **78**, 064301 (2008)